Cancer Immunol Immunother
DOI 10.1007/s00262-012-1295-4

ORIGINAL ARTICLE

High lipid content of irradiated human melanoma cells does not affect cytokine-matured dendritic cell function

Gabriela A. Pizzurro · Florencia P. Madorsky Rowdo · Luciana M. Pujol-Lereis · Luis A. Quesada-Allué · Andrea M. Copati · María P. Roberti · Jean-Luc Teillaud · Estrella M. Levy · María M. Barrio · José Mordoh

Received: 27 December 2011 / Accepted: 29 May 2012

Abstract Gamma irradiation is one of the methods used to sterilize melanoma cells prior to coculturing them with monocyte-derived immature dendritic cells in order to develop antitumor vaccines. However, the changes taking place in tumor cells after irradiation and their interaction with dendritic cells have been scarcely analyzed. We demonstrate here for the first time that after irradiation a fraction of tumor cells present large lipid bodies, which mainly contain triglycerides that are several-fold increased as compared to viable cells as determined by staining with Oil Red O and BODIPY 493/503 and by biochemical analysis. Phosphatidyl-choline, phosphatidyl-ethanolamine and sphingomyelin are also increased in the lipid bodies of irradiated cells. Lipid bodies do not contain the melanoma-associated antigen MART-1. After coculturing immature dendritic cells with irradiated melanoma cells, tumor cells tend to form clumps to which dendritic cells adhere. Under such conditions, dendritic cells are unable to act as stimulating cells in a mixed leukocyte reaction. However, when a maturation cocktail composed of TNF-alpha, IL-6, IL-1beta and prostaglandin E2 is added to the coculture, the tumor cells clumps disaggregate, dendritic cells remain free in suspension and their ability to efficiently stimulate allogeneic lymphocytes is restored. These results help to understand the events following melanoma cell irradiation, shed light about interactions between irradiated cells and dendritic cells, and may help to develop optimized dendritic cell vaccines for cancer therapy.

Keywords Melanoma · Gamma irradiation · Dendritic cells · Lipids · Immunotherapy

Introduction

Dendritic cells (DC) are central to the functioning of the immune system, since they connect innate immunity and the initiation of antigen (Ag)-specific immune response. DC are professional Ag-presenting cells, with potent Ag-phagocytosis, Ag-processing and presentation capacities. Through modulation of these functions, DC may lead the immune system to a tolerogenic or to a highly reactive immunogenic state [1–5]. Despite the well-demonstrated function of DC in the defense against infections, their role in cancer immunity remains unclear. Although tumor Ag presentation by DC has been extensively studied in vitro [6, 7], the in vivo process is not completely understood. For a DC-based vaccine to be effective, at least three conditions must be fulfilled: (1) the Ag must be present in a suitable state for being captured and processed by DC,

Electronic supplementary material The online version of this article (doi:10.1007/s00262-012-1295-4) contains supplementary material, which is available to authorized users.

G. A. Pizzurro · A. M. Copati · M. P. Roberti · E. M. Levy · M. M. Barrio · J. Mordoh (✉)
Centro de Investigaciones Oncológicas-Fundación Cáncer, Instituto Alexander Fleming, Cramer 1180, 1426 Buenos Aires, Argentina
e-mail: jmordoh@leloir.org.ar

F. P. Madorsky Rowdo · L. M. Pujol-Lereis · L. A. Quesada-Allué · J. Mordoh
Fundación Instituto Leloir-IIBBA, CONICET, Av. Patricias Argentinas 435, 1405 Buenos Aires, Argentina

J.-L. Teillaud
INSERM UMR-S 872, Centre de Recherche des Cordeliers, Université Pierre et Marie Curie, Université Paris Descartes, 75006 Paris, France

Published online: 22 June 2012

(2) DC should be competent and act in a pro-immunogenic environment; and (3) DC must be able to mature and travel to the lymph nodes to prime naïve lymphocytes. One of several approaches for Ag-loading DC in cancer vaccination has been to use whole tumor cells as Ag source, thus exposing DC to a full repertoire of known and unknown Ag. Recent genomic work performed in human cutaneous melanoma (CM) and in the murine melanoma cell line B16F10 revealed the presence of dozens of mutations in the CM genome, many of them residing in exons and giving origin to immunogenic peptides [8–10]. However, DC loaded with tumor cells may induce tolerogenic or immunogenic responses [2, 11–14]. When this approach is used, the replicative ability of tumor cells must be abolished before exposing them to DC, and the most common sterilization methods are cell lysis [15] or gamma irradiation (RT) [16–18]. Although many studies have utilized this approach, the analysis of biochemical and cytological changes produced in tumor cells after RT, as well as the Ag fate, has received little attention. In the human setting, we have previously used allogeneic RT cells to immunize CM patients, adding BCG as a TLR4 ligand and GM–CSF [19] to attract DC to the vaccination site [22]. The RT cells used for vaccination showed striking morphological changes, including the presence of large vacuoles, suggesting changes in their lipidic composition. We have also used as a vaccine monocyte-derived DC cocultured with a mixture of RT allogeneic melanoma cells (DC/Apo-Nec vaccine). This vaccine proved to efficiently cross-present the melanoma-associated Ags MART-1 and gp100 to specific CD8 T cell clones [18]. DC/Apo-Nec vaccine Phase I trial on 16 CM patients demonstrated that whereas 80 % of stages II and III vaccinated patients had an updated disease-free survival longer than 8 years, stage IV patients had progressive disease [16]. Thus, the immune protection induced with the DC/Apo-Nec vaccine could apparently cope with microscopic metastases, but not with bulky disease. It appears therefore of importance to better understand the interactions between DC and RT tumor cells to improve vaccine efficiency. It has been recently reported that DC from mice bearing different types of tumors have higher amount of lipids, mainly triglycerides (TG), than DC from naïve mice, and that such lipid-laden DC are less efficient to process Ag [20]. Therefore, it seemed important to consider if such situation was taking place in our vaccination system. In this work, we have focused on three major points: (1) to investigate whether RT affects the lipid composition of melanoma cells; (2) to analyze if DC maturation and functionality are altered after exposure to RT tumor cells; (3) to monitor the fate after RT of the melanocytic differentiation Ag MART-1 [21].

Materials and methods

Cell lines

MEL-XY1, MEL-XY2 and MEL-XY3 cell lines were grown as previously described [16, 18, 22].

Cell RT

Viable melanoma cell lines were RT at 25 or 70 Gy and frozen as described [18].

Cell viability and apoptosis

RT cells were thawed and plated in p35 plates (TPP, Germany) in fresh serum-free AIM-V^{TM} Medium (Therapeutic grade, GIBCO, Invitrogen Corporation, Grand Island, NY) at 1.0×10^6 cells/ml to complete the apoptosis–necrosis process. After 0, 6, 24, 48 and 72 h incubation at 37 °C, the cells were detached by repeated pipetting. Cell number and viability were measured by Trypan-Blue exclusion. Apoptosis and necrosis were assessed by flow cytometry (FACSCalibur, BD Biosciences, San Jose, CA) using Annexin-V/Propidium Iodide (AnnV/PI) (Annexin-V Apoptosis Detection kit, BD Biosciences, San José, CA) following the manufacturer's recommendations. The viable, necrotic and apoptotic/necrotic (Apo/Nec) cell populations were expressed as percentages of total events, and viable cells were used as controls. Cell viability was also determined by MTT as previously described [23].

Percoll gradient centrifugation

Seventy Gy RT cells were separated in a Percoll gradient as described [24].

Cytochemical detection of lipids

Oil Red O (ORO) staining was performed on viable and RT cells. Cell pellets from each condition were fixed in 3 % paraformaldehyde (PFA), and a drop of the suspension was placed on glass slides and air-dried. The slides were washed twice with water, once with polyethylenglycol (PEG) and stained at 60 °C for 10 min with a 0.5 % solution of ORO (Sigma Chemical Company) in PEG. The slides were washed with 85 % PEG, counterstained with hematoxylin, washed with tap water and mounted with glycerol. Observations were performed with a Zeiss Axioplan microscope, and the images were recorded with a DP72 Olympus digital camera. Alternatively, 0.5×10^6 cells were incubated with 200 µl of 10 µg/ml BODIPY 493/503 (4,4-difluoro-1,3,5,7,8-pentamethyl-4-bora-3a,4a-diaza-s-indaceno, Molecular Probes, Invitrogen) in PBS for

15 min at room temperature, washed and fixed in 1 % PFA. Samples were mounted and analyzed as before.

Lipid content determination by flow cytometry

RT cells were detached by pipetting at the indicated times, centrifuged, washed with PBS, and 0.5×10^6 cells were stained with 200 µl 0.5 µg/ml BODIPY 493/503 in PBS for 15 min at room temperature. The cells were washed, fixed in 1 % PFA, washed again and analyzed by flow cytometry as described before. Viable cells were used as controls.

Isolation of lipid bodies (LB)

100×10^6 MEL-XY3 viable cells were obtained as described before, and 100×10^6 MEL-XY3 RT cells were thawed and allowed to apoptotize during 48 h. After centrifugation at 1,500 rpm for 5 min, cells were resuspended in 6 ml disruption buffer (0.25 M sucrose, 20 mM Tris–HCl buffer pH7.4, 1 mM EDTA) with the addition of 30 µl of the protease inhibitor cocktail P8340 (Sigma-Aldrich, USA). Cell suspensions were disrupted at 4 °C with a Dounce homogeneizer (4 cycles of 20 strokes separated by a 1-min interval). RT cells were further disrupted with a Polytron homogeneizer (IKA Werke, GMBH, Germany) (4 rounds, 30 s each round, at 4 °C). Both homogenates were centrifuged at 12,000 rpm for 10 min, and the supernatants (S1) were diluted to 10 ml with 20 mM Tris–HCl pH7.4: physiological solution (1:1). The supernatants were centrifuged at 100,000×*g* for 1 h at 4 °C. Aliquots were saved for protein determination. After centrifugation, the top layer of lipid cake was separated and frozen at −80 °C in glass tubes until further processing.

Biochemical analysis

MEL-XY3 LB obtained from 25×10^6 viable or 48 h RT cells were lyophilized and resuspended in chloroform:methanol 3:2 for 30 min. After centrifugation at 7,000 rpm for 30 min to eliminate insoluble material, the samples were partitioned, washed with 4 mM $MgCl_2$ according to Folch [25], and the lower lipidic phase was dried at 40 °C under gaseous nitrogen. For TLC separation, Silica Gel 60 TLC plates (Merck) were prewashed with chloroform and activated prior to use. A fraction of the sample corresponding to 6×10^6 cells was used to separate neutral lipids using a one-dimensional, three-solvent system as follows: (1) hexane to the top; (2) toluene to the top; (3) hexane: diethyl ether: acetic acid (70:30:1) 12 cm from the origin [26]. The plates were sprayed with ferric chloride/sulfuric acid solution and heated at 180 °C. Polar lipids corresponding to 3×10^6 cells were also analyzed. In this case, the plates were developed by a one-dimensional, two-solvent system as follows: (1) chloroform:methanol: acetic acid:water (40:10:10:1); (2) chloroform: methanol: acetic acid: water (120:46:19:3) [27]. Plates were sprayed with 5 % ethanolic phosphomolybdic acid solution, heated at 180 °C, and exposed to ammonia vapors to whiten the background. Densitometry was performed using the ImageJ program. Standards were 1,2-dipalmitoyl-sn-glycerol and monomyristin (Echelon Biosciences Inc., Salt Lake City, UT, USA), coenzyme Q1, squalene,L-α-phosphatidylcholine, L-α-phosphatidyl-L-serine, L-α-phosphatidyl-ethanolamine, L-α-lysophosphatidylcholine, cholesterol-palmitate, glyceryl-trioleate, stearyl-arachidate, methyl-palmitate, cardiolipin, 1-(3-*sn*-phosphatidyl)-*rac*-glycerol, oleic acid and cholesterol (Sigma-Aldrich) and dolichol (Avanti Polar Lipids Inc., Alabaster, AL, USA). All solvents used were HPLC grade.

DNA synthesis

0.2×10^6 viable or RT MEL-XY3 cells/well were plated in a 96-well plate in 200 µl of melanoma medium (MM) + 10 % fetal bovine serum (FBS) (Natocor, Argentina) [22]. Viable cells were incubated overnight, whereas RT cells were incubated for the indicated times. After performing a 2-h pulse with 1 µCi/ml [^{3}H]thymidine ([^{3}H]dThd) (Perkin Elmer, Boston, USA), the cells were harvested with a Nunc Cell Harvester 8 (Nalge Nunc International Corp. USA), and the incorporated radioactivity was determined with a Liquid Scintillation Counter (Wallac 1214 Rackbeta, Pharmacia).

Fatty acid synthesis

0.8×10^6 viable or RT MEL-XY3 cells/well were plated in 0.8 ml of MM + 10 % FBS in a 24-well plate, and a 2-h pulse with 1 µCi/ml [1,2 ^{14}C]acetic acid (Perkin Elmer, Boston, USA) was performed. The cells were detached, washed and frozen at −80 °C in glass tubes until further processing. The samples were resuspended in chloroform:methanol 3:2, centrifuged at 7,000 rpm for 30 min, and the lipidic extracts were processed and the incorporated radioactivity quantified as above. TLC was performed to analyze label incorporation into neutral lipids. The plates were exposed on imaging storage phosphor screens, and these were scanned with a STORM 840 (Molecular Dynamics Division, Amersham Pharmacia Biotech). The plates were sprayed with ferric chloride/sulfuric acid solution and heated at 180 °C to detect lipids. To inhibit fatty acid synthesis, C75 [4-methylene-2-octyl-5-oxo-tetrahydrofuran-3-carboxylic acid] (Cayman Chemical Company, USA) was used as previously described [28].

MART-1 and lipid bodies colocalization

1.0×10^6 viable or RT cells were fixed in 200 µl 3 % PFA during 10 min, permeabilized with 200 µl 0.05 % saponin in PBS (PBS-SAP) for 15 min at room temperature, washed once in PBS-SAP and incubated 45 min at 4 °C with 200 µl of 5 µg/ml anti-MART-1 2A9 mAb in PBS-SAP. 2A9 mAb is an in-house produced IgG1 mAb which was labeled with AlexaFluor^{647} (2A9 AF647) (Invitrogen). After washing, BODIPY 493/503 staining was performed. Finally, the cells were washed in PBS, resuspended in Mowiol (Polysciences Inc., USA), mounted on glass slides and observed with a confocal microscope (Carl Zeiss, LSM 510, Meta). The AIM Carl Zeiss software was employed to analyze the data.

MART-1 western blot

Cells were centrifuged, washed with PBS and resuspended in lysis buffer (10 mM Tris–HCl pH 8, 1 % Triton X-100, 50 mM NaCl, 5 mM EDTA and 1/200 protease inhibitor cocktail (Sigma-Aldrich, USA) at 50 µl per 1.0×10^6 cells). Protein determination was performed as described [29]. Ten microliters of cell extracts were ran in a 12 % SDS-PAGE gel and transferred to nitrocellulose membranes (Immobilon, 0.45 µm pore size, HATF 304 FO, Millipore, USA). After blocking in 3 % skimmed milk in PBS, the blots were incubated with 5 µg/ml anti-MART-1 2A9 mAb and 0.8 µg/ml anti-beta-actin mouse IgG2a (Sigma-Aldrich, USA). After washings, blots were further incubated with 1/2,500 alkaline phosphatase-AffiniPure F(ab')2 Fragment Goat Anti-Mouse IgG (H + L) (Jackson ImmunoResearch, USA) and developed with nitroblue tetrazolium/5-bromo-4-chloro-3-indolyl-phosphate (NBT-BCIP) (Promega, USA).

Generation of immature DC (iDC) from peripheral blood

Human DC were derived from PBMC of buffy-coats obtained from healthy donors at the Hemotherapy Department of the Instituto Alexander Fleming as previously described [14]. This procedure received approval from the Institutional Review Board of the Instituto Alexander Fleming, and healthy donors gave written informed consent.

DC maturation and coculture with RT cells

RT cells were prepared under two different conditions: (1) they were thawed immediately before coculture with iDC (Apo-Nec T0); (2) they were thawed and plated to undergo apoptosis during 72 h in AIM-V^{TM}, washed twice in PBS and then cocultured with iDC (Apo-Nec T72). Five-days iDC were cocultured for 48 h with Apo-Nec T0 (DC/Apo-NecT0) or Apo-Nec T72 (DC/Apo-NecT72) in p35 plates with AIM-V^{TM} Medium in a 3:1 iDC:Apo-Nec ratio. Alternatively, a cytokine maturation cocktail containing 10 ng/ml TNF-alpha, 10 ng/ml IL-1beta, 100 ng/ml IL-6 (Peprotech, México) and 1 µg/ml PGE-2 (Calbiochem, Argentina) was added to the cocultures. Controls of DC maturation were performed by adding 2 µg/ml LPS (Lipopolysaccharide from *E. coli* J5, Sigma-Aldrich, USA) or maturation cocktail alone to iDC for 48 h. DC markers were measured as described [18]. For CD86 staining, DC were incubated with anti-CD86-PE (BD Biosciences, San Jose, CA) for 30 min at 4 °C, fixed with 3 % PFA, mounted in Mowiol and observed with an Axioplan Zeiss microscope.

Mixed leukocyte reaction (MLR)

DC/Apo-NecT0 and DC/Apo-NecT72, obtained after 48 h coculture with or without maturation cocktail, were resuspended by gentle pipetting, washed in PBS and treated with 15 ug/ml mitomycin C (Delta Farma, Buenos Aires, Argentina) in AIM-V^{TM} Medium for 3 h at 37 °C. The cells were then washed twice in excess PBS and used as stimulator cells. Effector allogeneic PBMCs were obtained from fresh blood by Ficoll-Hypaque gradient centrifugation. MLR cocultures were performed in quadruplicate in flat-bottom 96-well plates in 200 µl AIM-V^{TM} Medium. Three different stimulator:effector ratios were used (1:10, 1:100 and 1:1000), maintaining effectors constant at 3×10^5 cells/well. After 4 days at 37 °C, 0.5 µCi per well [^{3}H]dThd were added and incubated overnight. After incubation, cells were processed as described in the metabolic labeling section. As a proliferation control, PBMC were incubated with 0.5 % phytohemagglutinin (PHA) (GIBCO, Invitrogen, USA) during 72 h before the [^{3}H]dThd pulse.

Protein content

It was measured as described by Bradford [29].

Results

Cell viability after RT

Viability, apoptosis and necrosis of MEL-XY3 cells were analyzed by Trypan-Blue exclusion and flow cytometry after AnnV/PI staining at different times after 25 and 70 Gy RT. The cell viability was rapidly lost, since at 0, 6, 24, 48 and 72 h after 70 Gy RT, viabilities were 50, 40, 25, 15 and 10 %, respectively. DNA synthesis was completely

abolished immediately after RT ($p < 0.001$). The results obtained with the MEL-XY3 cell line were representative of the different cell lines and are shown in Online Resource 1a. It is noteworthy that although the total number of RT cells only dropped to 65 % at 72 h, the cellular protein content fell to 30 %, indicating that RT cells leaked most of their protein. When apoptosis/necrosis was analyzed by flow cytometry (Online Resource 1b), we observed that whereas basal apoptosis and necrosis in exponentially growing cultures were about 10 %, levels of both early apoptotic ($AnnV^+PI^-$) and secondary necrotic ($AnnV^+PI^+$) cells increased to approximately 30 % immediately after 70 Gy RT and then rapidly progressed to 70, 80 and 90 % at 24, 48 and 72 h, respectively. After 96 h, 87 % of the cells had undergone secondary necrosis, and 7 % had lost AnnV-binding capability. Even after completely losing the capacity of DNA synthesis and the ability to grow in soft agar clonogenic assays (data not shown), the percentage of $AnnV^-PI^-$ cells after RT was about 50 % at 0 h and then rapidly decreased to less than 1 % 96 h after RT, the last evaluated time. Thus, RT cells contained a mixture of necrotic, apoptotic and non-apoptotic, non-proliferating cells. Similar results were obtained for MEL-XY3 after 25 Gy RT (Online Resource 1b).

Large lipid bodies are formed after RT

After RT, the cells underwent progressive changes in their morphology, with bubbling of the plasma cell membranes and progressive detection of an elevated number of cytoplasmic large spherical droplets, suggestive of lipid content. To determine whether such droplets had a lipidic composition, two staining methods were used. First, we stained with ORO [30] Mel-XY3 cells, either viable or at different times after RT. In Fig. 1a (left), it could be observed that viable cells contained a small amount of lipid bodies and a diffuse cytoplasmic staining. Starting 6 h after RT, a fraction of the cells presented in their cytoplasm large lipid-containing structures, named hereafter radiation-induced lipid bodies (RILB) (data not shown). Such content increased dramatically 48 h after RT, when most of the cells were loaded with RILB (Fig. 1a, middle and right). At 72 h, this percentage decayed and most of the lipid droplets were attached to the plasma membrane or extruded from the cells. We also observed that after RT the cells tended to clump in moderate size aggregates.

Since similar results were observed with Mel-XY1 and Mel-XY2, we continued our work on MEL-XY3. ORO staining suggested that RT cells were enriched in RILB, apparently containing neutral lipids. To confirm this observation, viable and Apo-Nec cells were stained with BODIPY 493/503, a specific dye for neutral lipids. An exact colocalization between refringent vacuoles observed under phase microscopy and BODIPY 493/503 staining was observed (Fig. 1b). To quantify LB, cells stained with BODIPY 493/503 were analyzed by flow cytometry (Fig. 1c), and it was found that staining increased progressively after RT, attaining a maximum at 48 h after RT, when around 40 % of the cells were positive, and then decreased. It should be noted that not every RT cell was high-stained with BODIPY, demonstrating heterogeneity in the neutral lipid content of the RT cell population.

Biochemical analysis of lipid bodies from viable cells (LB) and RT cells (RILB)

To compare the biochemical nature of LB of viable cells and RILB of RT cells, they were isolated from MEL-XY3 cells at two different conditions, viable and 48 h after RT and analyzed by TLC to characterize their neutral lipid and phospholipid content. As described under "Materials and methods", RT cells were remarkably more resistant to disruption than viable cells. TLC for neutral lipids showed that, both in viable and RT cells, most of them were TG (Fig. 2a, b); when TG level was referred to protein content of the S1 supernatants, it was twice in RT than in viable cells (Fig. 2c). After correcting for protein content, free-cholesterol (FC) also increased in RT cells, while cholesterol esters (CE) remained unchanged.

Phospholipids were identified as phosphatidyl-ethanolamine (PE), phosphatidyl-choline (PC), sphingomyelin (SM), lysophosphatidyl-choline (LPC), phosphatidyl-inositol (PI), and phosphatidyl-serine (PS) (Fig. 2d). When phospholipid content was adjusted for protein content, RT cells possessed three-fold content of PE and PC, and twofold content of SM and PI than viable cells. In contrast, LPC was slightly reduced in RT cells.

The increase in lipid content, and number and size of RILB in RT cells, could be explained either by fusion of already existing lipid bodies or by de novo synthesis. Using [^{14}C]acetic acid as a precursor, we determined that RT cells were able to synthesize lipids, although at a much lower rate than viable cells (Fig. 2g). When labeled lipids were analyzed by TLC, it was shown that RT cells synthesized TG and phospholipids (Fig. 2i), and that in spite of a much lower de novo TG synthesis in RT cells, they contained a higher TG content than viable cells (Fig. 2h). These results argue against de novo lipid synthesis in RT cells as the main contributor to TG increment, suggesting that redistribution of pre-existing lipids could take place to generate RILB.

Inhibition of lipid synthesis with C75

In an attempt to analyze the possible role of RILB in Apo/Nec RT cells in regard to their interaction with DC, it

would have been desirable to obtain a cellular subpopulation containing RILB and another lacking them. We first investigated whether inhibition of lipid synthesis diminished the number of LB in CM cells. For this, viable Mel-XY3 cells were treated with C75 an inhibitor of fatty acid synthase (FAS), a key enzyme in lipid metabolism, which expression is increased in different types of cancer [31]. First, an MTT assay was performed to study the cytotoxicity of the inhibitor. An important reduction in cell viability was observed starting at 10–20 μg/ml C75 (Online Resource 2a). We confirmed that the cells were rendered Apo/Nec by AnexinV/IP assay (Online Resource 2d, 2e). The effect of C75 on LB formation was analyzed by BODIPY 493/503 staining. No significant differences in LB number per cell were observed after C75 treatment, although those numbers were quite variable. Only after a 6-h treatment with 50 μg/ml C75 treatment, a reduction in LB was observed, but most cells died at that concentration (Online Resource 2b). Inhibition of lipid synthesis after C75 treatment was also analyzed by [^{14}C]acetic acid incorporation. A significant decrease in [^{14}C]acetic acid incorporation was only observed at 20 and 50 μg/ml of C75 (Online Resource 2c), both doses being lethal for CM cells.

Since we had observed that some RT Mel-XY3 cells presented RILB while other cells did not (Fig. 1), we tried to isolate cells with different lipid content by using Percoll gradients. However, the cells were separated according to their nucleus/cytoplasm ratio rather than by their lipid content (data not shown).

Expression and localization of MART-1 in melanoma cells at different times after RT

Since dramatic changes in cell viability and formation of RILB took place in RT cells, it was important to determine the fate of the melanoma-associated Ag MART-1, an early tumor rejection Ag [21]. Western blots were performed to assess MART-1 stability at different times (0–72 h) after RT. Figure 3a shows that, although RT of melanoma cells determines a decrease in total protein, as determined by beta-actin content, MART-1 was clearly enriched, attaining in several experiments an average of twofold level increase (data not shown) 72 h after RT. Since in viable cells, MART-1 is associated with the lipid membranes of melanosomes [32], it was of interest to determine whether it colocalizes with RILB. LB were therefore labeled with BODIPY 493/503 and MART-1 with 2A9 AF647, and the dual staining was analyzed by confocal microscopy (Fig. 3b). In some tumor cells, MART-1 was diffusely dispersed in the cytoplasm, whereas in other cells, it was also found concentrated in perinuclear granules. However, either in viable or RT cells, regardless the time after RT tested, no colocalization was observed between LB, RILB and MART-1.

Fig. 1 ORO and BODIPY 493/503 staining of viable and RT melanoma cells. **a** MEL-XY3 cells were stained with ORO as described under "Materials and methods". *Middle panel* shows phase contrast microscopy. Original magnification: ×1,000. **b** MEL-XY3 6 h (*i*) or 24 h (*iii*) after RT were stained with BODIPY 493/503 as described under "Materials and methods". *ii* and *iv* are the corresponding phase contrast pictures. Original magnification: × 1,000. **c** BODIPY 493/503 staining was analyzed by flow cytometry and fluorescence microscopy in viable cells and at different times after RT. Results are shown as a *dot* plot with a representative picture. Flow cytometry data are also plotted in an histogram showing a clear separate high lipid-containing-cell population after RT. Percentages of high lipid-containing cells are shown. *SSC* side scatter

DC/Apo-Nec cells contain RILB

In order to investigate whether DC submitted to different maturation stimuli differed in their lipid content, Apo-Nec cells, iDC, LPS-matured DC and DC/Apo-NecT0 cells were stained for lipids with BP 493/503. We also determined whether MART-1 was transferred from RT tumor cells to DC during coculture. DC were detected with CD86-PE and MART-1 with the 2A9 AF647 mAb. The results, shown in Online Resource 3, showed that DC from DC/Apo-Nec cocultures had larger and distinct RILB than iDC or LPS-matured DC. Traces of MART-1 were also detected within DC in DC/Apo-Nec, demonstrating uptake of the Ag. To analyze if RILB were incorporated by DC as vesicles, Apo-Nec cells were labeled with BODIPY 493/503 before coculture. When DC/Apo-Nec were analyzed, no label was found within DC (data not shown).

Effect of lipid-containing RT tumor cells on DC stimulating capacity in mixed leukocyte reaction

It has been reported that lipid uptake by DC may affect their function [20]. Since tumor cells progressively increase their lipid content after RT (see Fig. 1), and DC from cocultures contain more LB than LPS-matured DC (Online Resource 3), we wanted to determine whether iDC exposure to RT tumor cells containing different amounts of RILB affected their function. Since RILB content increased after RT, reaching a peak at 48 h and decreasing by 72 h (Fig. 1), it could be hypothesized that iDC exposed to Apo-NecT0 might capture higher amount of lipids than iDC exposed to Apo-NecT72. To investigate DC function under both conditions, mixed leukocyte reactions (MLR), a standard test to analyze DC stimulating ability [33], were performed. At a 10:1 effector:stimulator ratio, only LPS-matured DC (DC + LPS) could stimulate effector cells, whereas DC/Apo-NecT0 or T72 barely stimulated

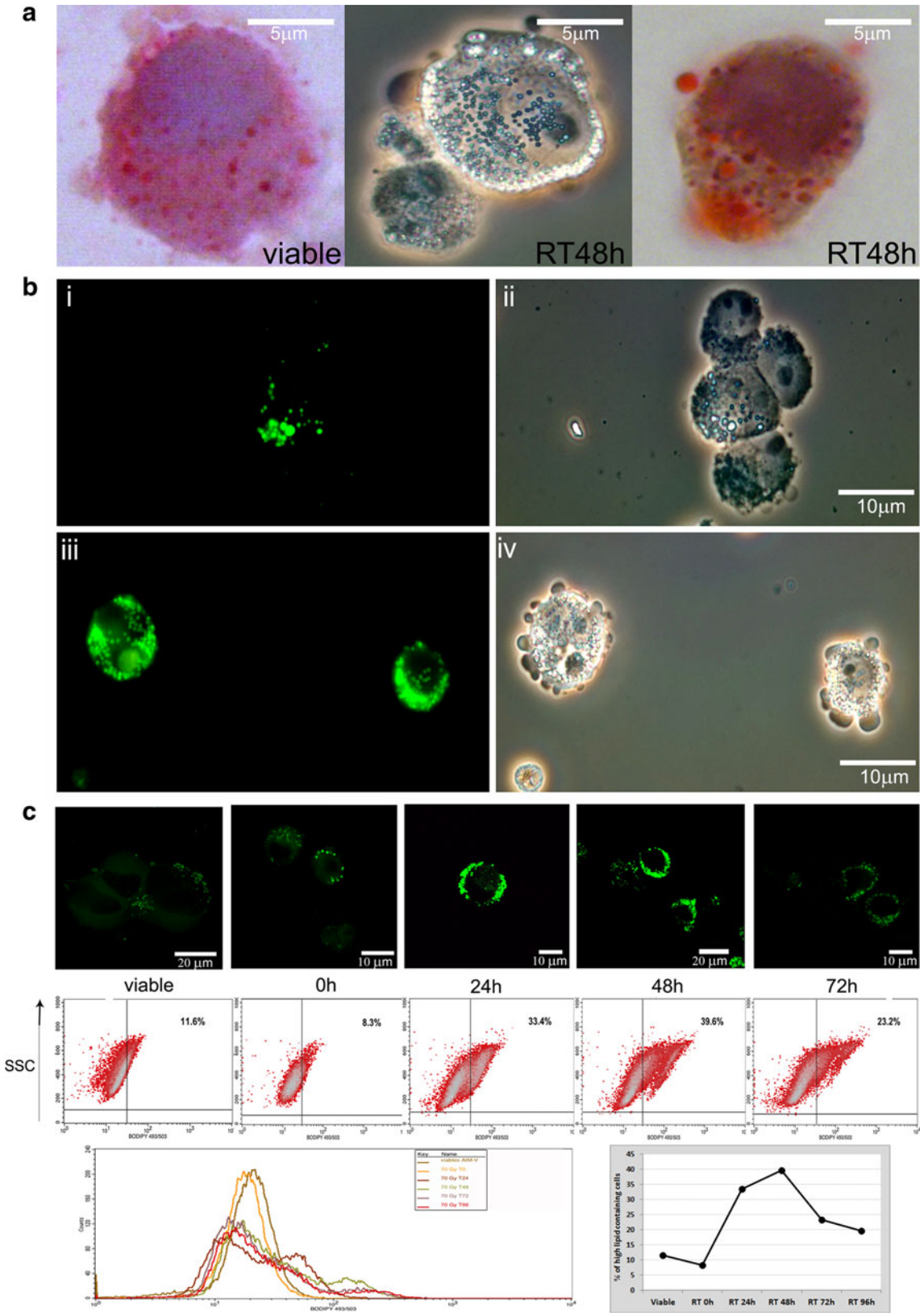
a
5μm
viable
5μm
RT48h
5μm
RT48h
b
i
ii
10μm
iii
iv
10μm
c
20 μm
10 μm
10 μm
20 μm
10 μm
viable
0h
24h
48h
72h
SSC
11.6%
8.3%
33.4%
39.6%
23.2%
BODIPY 493/503
% of high lipid containing cells
Viable
RT 0h
RT 24h
RT 48h
RT 72h
RT 96h

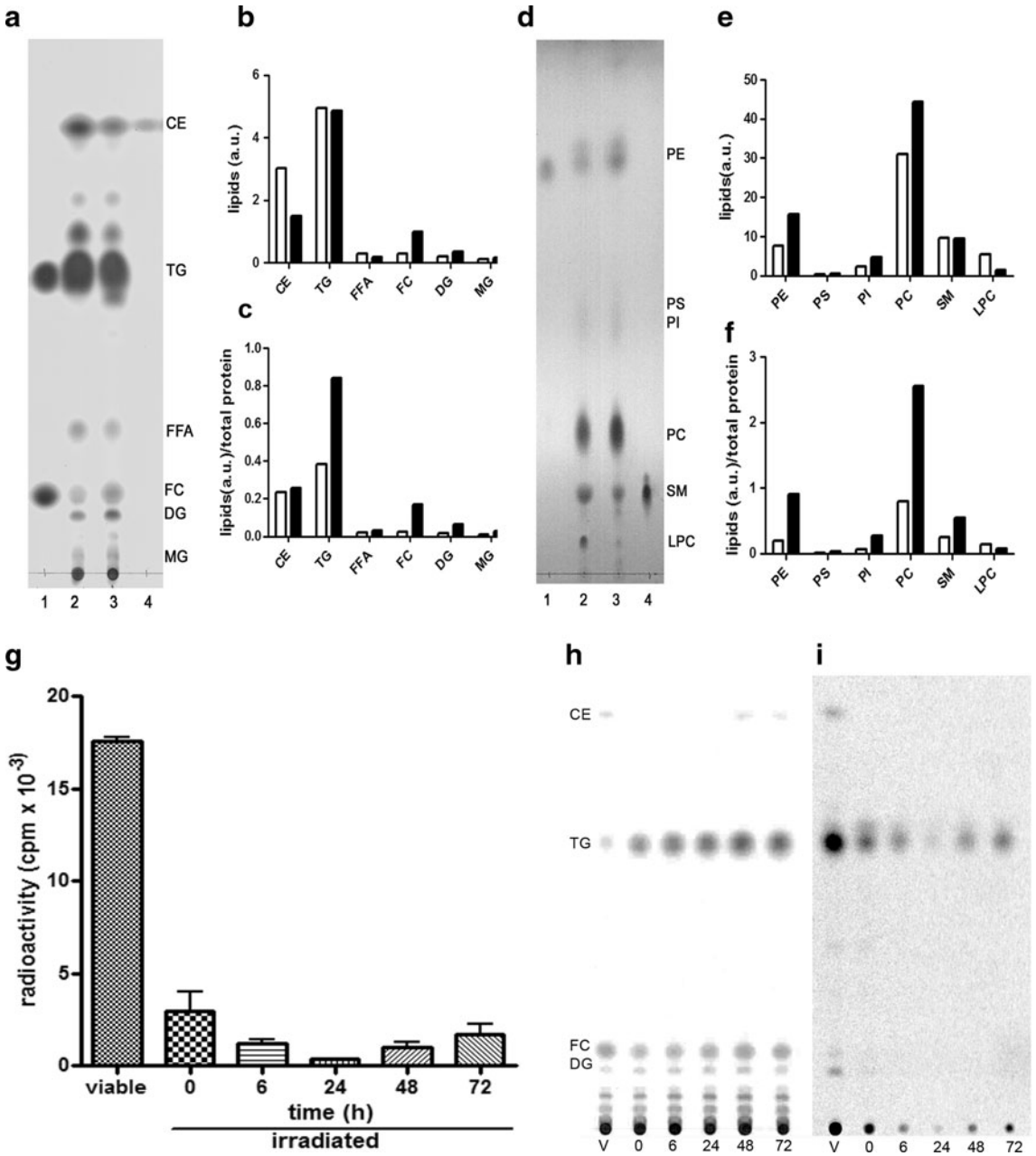

Fig. 2 Lipid composition and fatty acid synthesis of viable and RT MEL-XY3. Lipid bodies were purified, and a lipid extraction and TLC were performed as described under "Materials and methods". **a** Neutral lipids TLC. *Lane 1* triolein + cholesterol standards (10 μg); *lane 2* viable cells; *lane 3* RT cells; *lane 4* cholesterol-palmitate standard (1 μg). **b** Densitometry histogram of (**a**). **c** Densitometry histogram of (**a**) referred to total protein content. **d** Phospholipids TLC. *Lane 1* PE standard; *lane 2* viable cells; *lane 3* 48 h RT cells; *lane 4* SM standard. **e** Densitometry histogram of (**d**). **f** Densitometry histogram of (**d**) referred to total protein. *Open bars*: viable cells, *black bars*: RT cells. **g** Fatty acid synthesis in whole cells. Cultures of viable and RT MEL-XY3 cells were pulse-labeled with [^{14}C]acetic acid as described under "Materials and methods". Results are shown as mean ± SD of two independent experiments. **h** TLC. *Lane 1* total lipids extracted from viable cells; *lanes 2–6* total lipids extracted from RT cells at 0, 6, 24, 48 and 72 h, respectively. **i** Incorporated radioactivity of TLC showed in **h**

allogeneic lymphocytes (Fig. 4a). When tested at 100:1 and 1,000:1 ratios, all DC combinations were unable to trigger stimulation (data not shown). In view of these results, we investigated whether the addition of a maturation cocktail (MC) [34] increased the stimulating ability of DC. In the presence of MC composed of TNF-alpha, IL-6, IL-1beta and PGE-2, a robust MLR was obtained at a 10:1 ratio with DC, DC/Apo-NecT0 or DC/Apo-NecT72 cells (Fig. 4a). Therefore, under the present experimental conditions, the different RILB content present in Apo-NecT0 or T72 cells did not affect the stimulating ability of MC-matured DC. However, when the DC markers HLA-II,

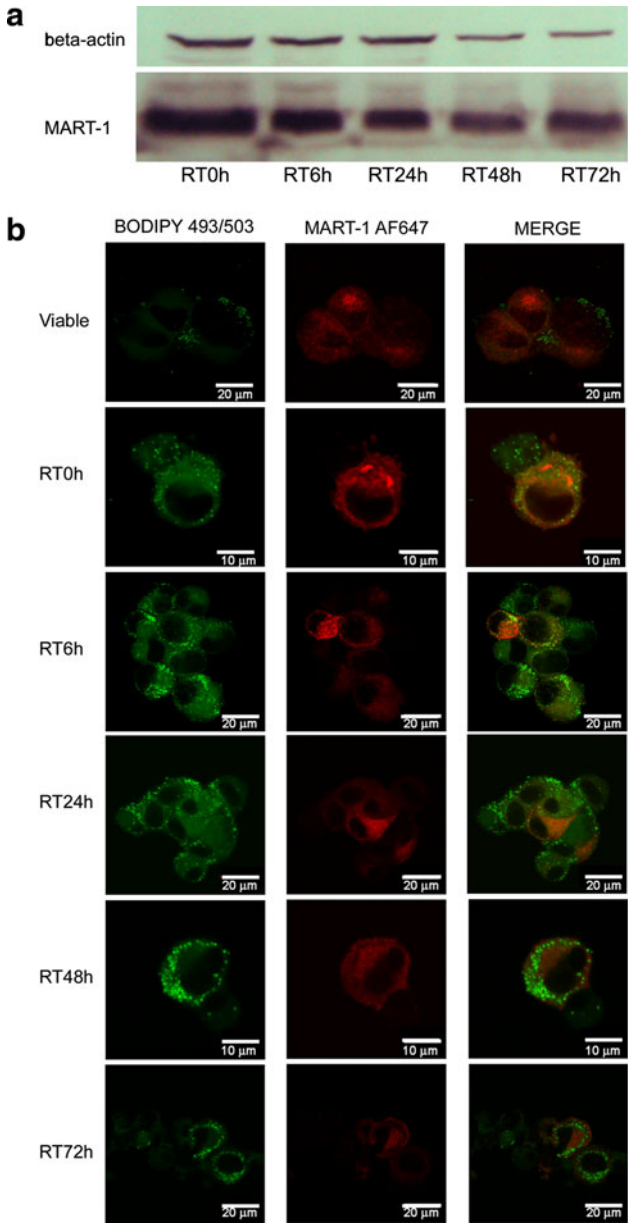

Fig. 3 MART-1 shows stability after RT and no colocalization with LB. **a** MART-1 levels were determined by Western blots in viable and RT cells, showing increased levels after RT, compared to beta-actin. **b** LB and MART-1 were detected in viable and RT cells with BODIPY 493/503 and 2A9 AF647 mAb as described under "Materials and methods"

CD80, CD86 and CD83 were measured, a trend to a higher maturation in DC/Apo-NecT72 cells than in DC/Apo-NecT0 cells was observed, although the difference did not attain statistical significance. This trend was maintained when MC was added (Fig. 4b).

Since differences in the expression of DC maturation markers could not explain by themselves the lack of stimulation in MLR in the absence of MC, the DC/Apo-Nec cocultures were microscopically examined after labeling DC with anti-CD86-PE mAb. Striking differences in intercellular interactions were observed. In the absence of MC, Apo-Nec cells formed large clumps, with DC mostly attached at their periphery (Fig. 4c). Instead, when MC was added, no clumps of Apo-Nec cells were observed, and DC remained free in the cell suspension. Therefore, lack of MLR stimulating ability could be due to steric hindrance of DC trapped in the Apo-Nec clumps. To investigate whether regain of MLR stimulating ability had some correlate with RILB content, labeling DC/Apo-Nec cells for lipids with BODIPY 493/503, DC with CD86-PE and MART-1 with the 2A9 AF647 was performed (Fig. 5). It was observed that the addition of MC did not affect the amount of RILB observed within DC/Apo-Nec cells. However, DC/Apo-Nec cells plus MC clearly contained more MART-1 in their cytoplasm, suggesting higher uptake of Apo/Nec debris.

Discussion

When DC are loaded with tumor cells in order to manufacture vaccines, two main issues must be considered: safety and efficacy. With respect to safety, tumor cell lysates offer immediate destruction of the cells, but after incubation with DC, the suspension is generally centrifuged and non-captured proteins are lost [15, 35]. We prefer the use of RT tumor cells as Ag source, since tumor cell debris non-phagocytosed by DC would remain at the injection site, thus serving as an Ag depot. We have previously demonstrated that RT effectively sterilizes every tumor cell employed for vaccine preparation, as measured by clonogenic assay, the most sensitive method to detect cell survival [16, 18, 22]. In this work, we have closely analyzed the time course of some events taking place in tumor cells and their consequences on DC function. In the first place, we observed that 60 % of the cells lost viability 6 h after RT, and 80 % of the cells became necrotic after 24 h (Online Resource 1b). DNA synthetic ability was immediately curtailed after RT. However, although 48–72 h after RT most tumor cells had lost around 70 % of their protein content and underwent dramatic morphological changes, they did not disintegrate. Also, 2 days after RT, tumor cells formed clumps, containing from a few to several hundred cells. We did not observe major differences between RT with 25 or 70 Gy in the triggered Apo/Nec process (Online Resource 1a).

As it refers to the efficacy of DC vaccines when using RT tumor cells, we observed that during the Apo/Nec process, a noticeable event was the generation of large LB (RILB) in about 40 % of the cells. RILB were larger than LB observed in live cells, were frequently extruded from RT cells, and were mainly composed of TG, as

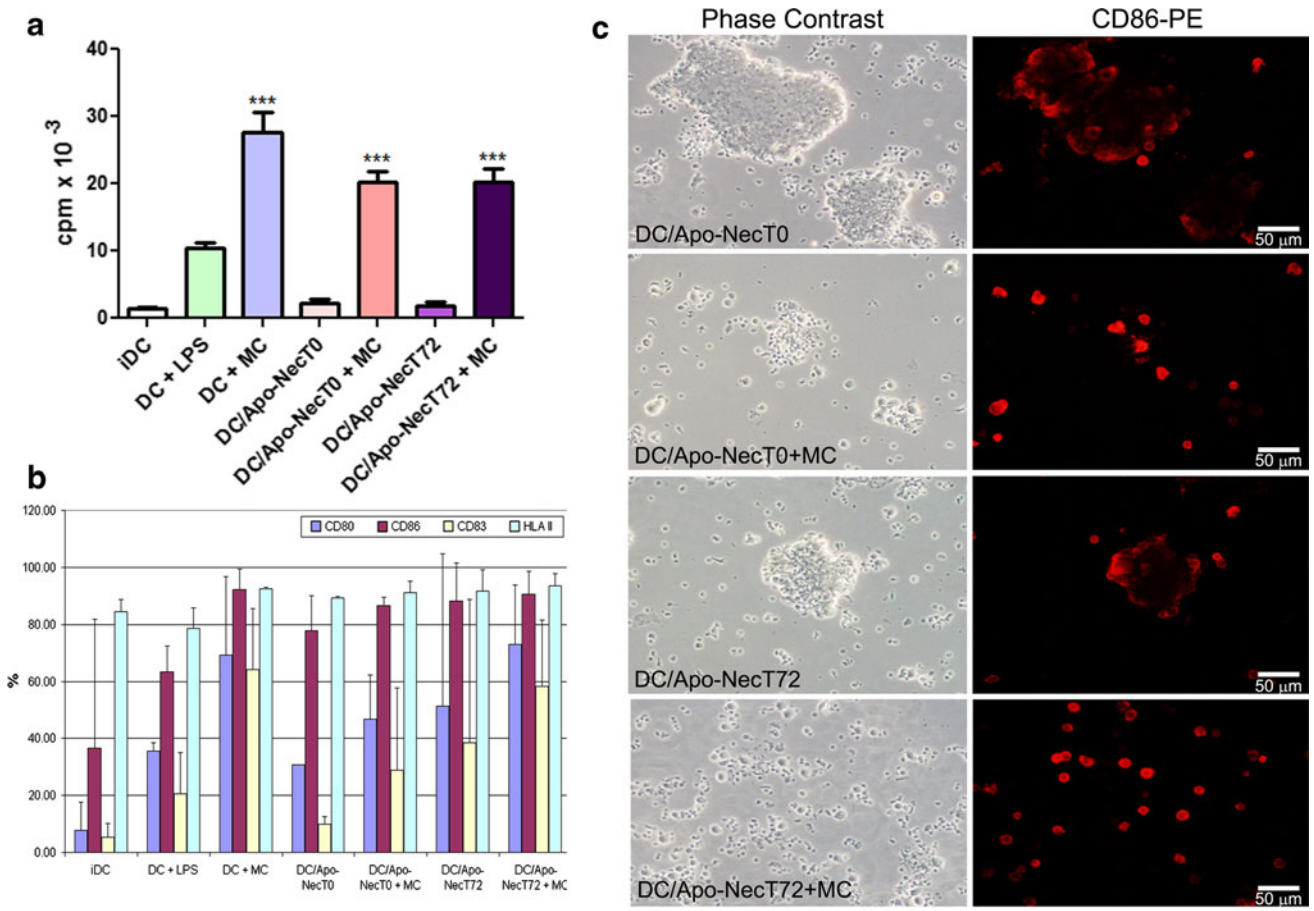

Fig. 4 Maturation and stimulating capacity of DC/Apo-Nec. **a** MLR. Different preparations of DC: Immature DC (iDC); LPS-matured DC (DC + LPS) or MC-matured DC (DC + MC); DC cocultured with Apo-Nec T0 cells in the absence (DC/Apo-NecT0) or presence of MC (DC/Apo-NecT0 + MC); DC cocultured with Apo-Nec T72 cells in the absence (DC/Apo-NecT72) or presence of MC (DC/Apo-NecT72 + MC). All were coincubated with allogeneic lymphocytes at 10:1 ratio for 4 days. The results shown are representative of three independent experiments performed. **b** DC maturation markers were analyzed by flow cytometry. Results represent the mean percentage obtained from DC of two independent healthy donors. **c** Phase and fluorescence microscopy of DC/Apo-Nec cocultures; DC were labeled with CD86-PE as described under "Materials and methods". Original magnification: × 400

demonstrated by staining with ORO, BODIPY 493/503 and biochemical analysis. Lipid bodies (LB), also known as lipid droplets, are newly recognised organelles formed by a neutral lipid core surrounded by a protein-bearing phospholipid monolayer. Originally believed to be inert energy storage bodies, recent evidence suggests that LB are highly dynamic organelles that participate in important cellular functions such as lipid metabolism and cellular energy homeostasis [36, 37]. Upregulated lipogenesis and increased number of LB were described in different types of human cancer cells [38–40], although their effect on tumor cell biology remains largely unknown [41]. The relation between LB, found in live cells, and RILB, found in RT cells, could not be determined. One possibility is that RILB are formed by the fusion of LB, since transition forms between LB and RILB were observed after RT (Fig. 1). In other systems, homotypic fusion events between LB have been observed [42], and it has been suggested that the SNARE (Soluble NSF Attachment Protein Receptor) system, composed of proteins that mediate vesicle fusion, could be involved in such events. An alternative explanation is de novo synthesis of RILB in RT cells. Although less incorporation of [^{14}C]acetic acid into lipids in RT cells than in viable cells took place, we propose that RILB formation includes multiple pathways besides de novo lipid synthesis, including lipids mobilization from other cellular compartments and capture of lipids released by dead cells to the medium. Al-Saffar et al. [43] showed that apoptosis in Jurkat cells is associated with TG accumulation, which occurred mainly in LB. They proposed that TG accumulation observed by ^{1}H-MRS and microscopy could be explained by an increase in PC catabolism or inactivation of PC synthesis. A drop in PC synthesis would produce an increase in diacylglycerol, which could be transformed to TG to avoid alteration of cellular metabolism [44]. The same hypothesis could be

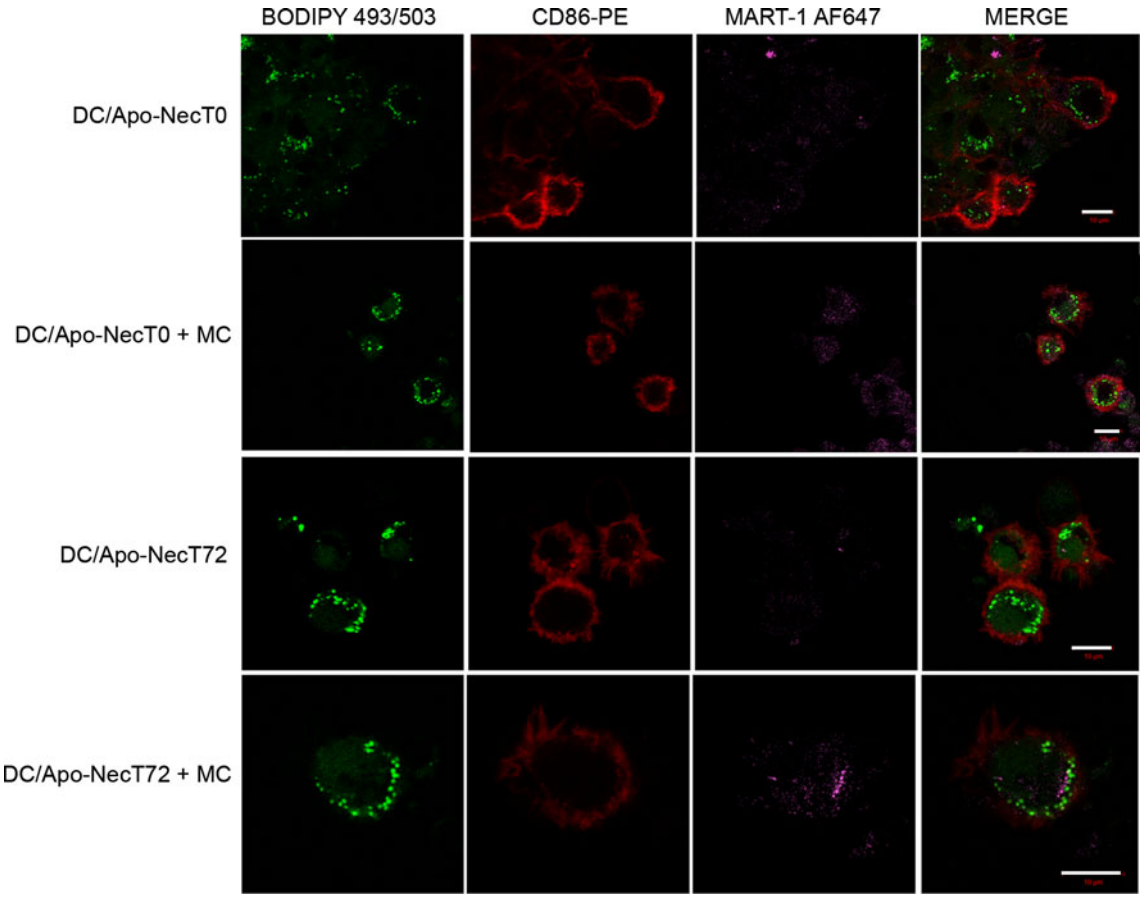

Fig. 5 Confocal microscopy analysis of LB and uptake of MART-1 in DC/Apo-Nec. DC/Apo-NecT0 or DC/Apo-NecT72 incubated in the absence or presence of MC were stained with BODIPY 493/503, CD86-PE and 2A9 AF647 as described under "Materials and methods". The addition of MC did not modulate the presence of RILB in neither DC/Apo-Nec. MART-1 uptake by DC was observed in all conditions. *Scale bar* 10 μm

also applied to our system, since when whole cells were analyzed, a reduction in PC was observed in RT cells (data not shown).

With regard to the efficacy of RT in the preservation of tumor Ags, we found that MART-1 was enriched in RT cells. A possible explanation would be that soluble proteins leak from RT cells more rapidly than membrane-bound hydrophobic MART-1. An alternative explanation could be a diminished proteasome activity induced by ionizing radiation [45]. Confocal microscopy analysis demonstrated that MART-1 was not associated with LB in viable cells or to RILB in RT cells. Also with respect to efficacy, it has been recently reported that DC from cancer-bearing mice have larger amounts of TG compared to those from normal mice, and that such DC would process Ag with lower efficiency [20]. Therefore, it was relevant to determine whether DC functionality would be diminished by the exposure to lipid-containing RT tumor cells. In the first place, we found that after being exposed to Apo-Nec tumor cells, DC appeared to contain larger amount of lipids than LPS-matured DC, suggesting that they had acquired lipids from phagocytosed Apo-Nec cells or from extracellular debris. Subsequently, to ascertain the physiological status of DC exposed or not to Apo-Nec cells, we analyzed their ability to stimulate allogeneic lymphocytes in MLR assays. The results clearly showed that DC exposed to Apo-Nec cells had negligible stimulatory capacity, even at a 10:1 effector:stimulator ratio, which was not due to a lack of HLA-I, HLA-II or costimulatory molecules (Fig. 4). However, such stimulatory capacity was fully regained when DC and Apo-Nec were cocultured in the presence of a MC composed of TNF-alpha, IL-6, IL-1beta and PGE-2, which increased further the expression of stimulatory and costimulatory molecules, and induced the disaggregation of homotypic clumps between RT cells. We propose that such clumps would be acting as a sink to DC, which would adhere to their surface and loose mobility for proper MLR to take place. It has been described [34] that the addition of MC increases motility of DC, which could therefore "escape" from the aggregates. The possibility of an increased secretion of proteases that could also cooperate to disaggregate clumps may not be excluded.

In conclusion, the present study demonstrates that important changes in lipid content took place in melanoma cells after RT. Such changes were accompanied by an increased amount of RILB, a new population of lipid bodies, and by a relative increase in TG. RILB were frequently extruded from the cell and were devoid of the MART-1 Ag. Most important, RILB did not diminish DC stimulating ability in the presence of a MC, which addition would allow the DC/Apo-Nec vaccine to fully exert its function. It remains to be established whether such functional enhancement includes DC traveling to lymph nodes and interaction with naïve lymphocytes.

Acknowledgments This work has been supported by grants from the Consejo Nacional de Investigaciones Científicas y Técnicas (CONICET), Agencia Nacional de Promoción Científica y Tecnológica (ANPCyT), Fundación Sales, Fundación Cáncer (FUCA), Fundación Pedro F. Mosoteguy, Fundación María Calderón de la Barca, Argentina and by INSERM (Institut National de la Santé et de la Recherche Médicale), by an Evaluation-Orientation de la Coopération Scientifique Sud (ECOS Sud)/Secretaría de Promoción Científica y Tecnológica (SEPCyT) exchange program grant (A03S03) from the Argentine SEPCyT and the French Ministère des Affaires Etrangères and by a grant from an INSERM/CONICET exchange program. JM, MMB, EML and LAQA are members of CONICET. FPMR, LMPL and MPR are fellows of the same Institution. GAP is a fellow of ANPCyT. JLT is a member of INSERM. AMC was supported by FUCA.

Conflict of interest The authors declare that they have no conflict of interest.

References

1. Banchereau J, Steinman RM (1998) Dendritic cells and the control of immunity. Nature 392(6673):245–252. doi:10.1038/32588
2. Steinman RM, Turley S, Mellman I, Inaba K (2000) The induction of tolerance by dendritic cells that have captured apoptotic cells. J Exp Med 191(3):411–416
3. Delamarre L, Mellman I (2011) Harnessing dendritic cells for immunotherapy. Semin Immunol 23(1):2–11. doi:10.1016/j.smim.2011.02.001
4. Palucka K, Ueno H, Banchereau J (2011) Recent developments in cancer vaccines. J Immunol 186(3):1325–1331. doi:10.4049/jimmunol.0902539
5. Green DR, Ferguson T, Zitvogel L, Kroemer G (2009) Immunogenic and tolerogenic cell death. Nat Rev Immunol 9(5):353–363. doi:10.1038/nri2545
6. Albert ML, Sauter B, Bhardwaj N (1998) Dendritic cells acquire antigen from apoptotic cells and induce class I-restricted CTLs. Nature 392(6671):86–89. doi:10.1038/32183
7. Ferlazzo G, Semino C, Spaggiari GM, Meta M, Mingari MC, Melioli G (2000) Dendritic cells efficiently cross-prime HLA class I-restricted cytolytic T lymphocytes when pulsed with both apoptotic and necrotic cells but not with soluble cell-derived lysates. Int Immunol 12(12):1741–1747
8. Chin L, Garraway LA, Fisher DE (2006) Malignant melanoma: genetics and therapeutics in the genomic era. Genes Dev 20(16):2149–2182. doi:10.1101/gad.1437206
9. Dutton-Regester K, Hayward NK (2012) Reviewing the somatic genetics of melanoma: from current to future analytical approaches. Pigment Cell Melanoma Res. doi:10.1111/j.1755-148X.2012.00975.x
10. Castle JC, Kreiter S, Diekmann J, Lower M, van de Roemer N, de Graaf J, Selmi A, Diken M, Boegel S, Paret C, Koslowski M, Kuhn AN, Britten CM, Huber C, Tureci O, Sahin U (2012) Exploiting the mutanome for tumor vaccination. Cancer Res. doi:10.1158/0008-5472.CAN-11-3722
11. Palucka AK, Ueno H, Connolly J, Kerneis-Norvell F, Blanck JP, Johnston DA, Fay J, Banchereau J (2006) Dendritic cells loaded with killed allogeneic melanoma cells can induce objective clinical responses and MART-1 specific CD8 + T-cell immunity. J Immunother 29(5):545–557. doi:10.1097/01.cji.0000211309.90621.8b
12. Nouri-Shirazi M, Banchereau J, Bell D, Burkeholder S, Kraus ET, Davoust J, Palucka KA (2000) Dendritic cells capture killed tumor cells and present their antigens to elicit tumor-specific immune responses. J Immunol 165(7):3797–3803
13. Berard F, Blanco P, Davoust J, Neidhart-Berard EM, Nouri-Shirazi M, Taquet N, Rimoldi D, Cerottini JC, Banchereau J, Palucka AK (2000) Cross-priming of naive CD8 T cells against melanoma antigens using dendritic cells loaded with killed allogeneic melanoma cells. J Exp Med 192(11):1535–1544
14. Michaud M, Martins I, Sukkurwala AQ, Adjemian S, Ma Y, Pellegatti P, Shen S, Kepp O, Scoazec M, Mignot G, Rello-Varona S, Tailler M, Menger L, Vacchelli E, Galluzzi L, Ghiringhelli F, di Virgilio F, Zitvogel L, Kroemer G (2011) Autophagy-dependent anticancer immune responses induced by chemotherapeutic agents in mice. Science 334(6062):1573–1577. doi:10.1126/science.1208347
15. Nestle FO, Alijagic S, Gilliet M, Sun Y, Grabbe S, Dummer R, Burg G, Schadendorf D (1998) Vaccination of melanoma patients with peptide- or tumor lysate-pulsed dendritic cells. Nat Med 4(3):328–332
16. von Euw EM, Barrio MM, Furman D, Levy EM, Bianchini M, Peguillet I, Lantz O, Vellice A, Kohan A, Chacon M, Yee C, Wainstok R, Mordoh J (2008) A phase I clinical study of vaccination of melanoma patients with dendritic cells loaded with allogeneic apoptotic/necrotic melanoma cells. Analysis of toxicity and immune response to the vaccine and of IL-10 -1082 promoter genotype as predictor of disease progression. J Transl Med 6:6. doi:10.1186/1479-5876-6-6
17. Neidhardt-Berard EM, Berard F, Banchereau J, Palucka AK (2004) Dendritic cells loaded with killed breast cancer cells induce differentiation of tumor-specific cytotoxic T lymphocytes. Breast Cancer Res 6(4):R322–R328. doi:10.1186/bcr794
18. von Euw EM, Barrio MM, Furman D, Bianchini M, Levy EM, Yee C, Li Y, Wainstok R, Mordoh J (2007) Monocyte-derived dendritic cells loaded with a mixture of apoptotic/necrotic melanoma cells efficiently cross-present gp100 and MART-1 antigens to specific CD8(+) T lymphocytes. J Transl Med 5:19. doi:10.1186/1479-5876-5-19
19. Dranoff G, Jaffee E, Lazenby A, Golumbek P, Levitsky H, Brose K, Jackson V, Hamada H, Pardoll D, Mulligan RC (1993) Vaccination with irradiated tumor cells engineered to secrete murine granulocyte-macrophage colony-stimulating factor stimulates potent, specific, and long-lasting anti-tumor immunity. Proc Natl Acad Sci USA 90(8):3539–3543
20. Herber DL, Cao W, Nefedova Y, Novitskiy SV, Nagaraj S, Tyurin VA, Corzo A, Cho HI, Celis E, Lennox B, Knight SC, Padhya T, McCaffrey TV, McCaffrey JC, Antonia S, Fishman M, Ferris RL, Kagan VE, Gabrilovich DI (2010) Lipid accumulation and dendritic cell dysfunction in cancer. Nat Med 16(8):880–886. doi:10.1038/nm.2172
21. Kawakami Y, Eliyahu S, Delgado CH, Robbins PF, Rivoltini L, Topalian SL, Miki T, Rosenberg SA (1994) Cloning of the gene

coding for a shared human melanoma antigen recognized by autologous T cells infiltrating into tumor. Proc Natl Acad Sci USA 91(9):3515–3519
22. Barrio MM, de Motta PT, Kaplan J, von Euw EM, Bravo AI, Chacon RD, Mordoh J (2006) A phase I study of an allogeneic cell vaccine (VACCIMEL) with GM-CSF in melanoma patients. J Immunother 29(4):444–454. doi:10.1097/01.cji.0000208258.79005.5f
23. Levy EM, Sycz G, Arriaga JM, Barrio MM, von Euw EM, Morales SB, Gonzalez M, Mordoh J, Bianchini M (2009) Cetuximab-mediated cellular cytotoxicity is inhibited by HLA-E membrane expression in colon cancer cells. Innate Immun 15(2):91–100. doi:10.1177/1753425908101404
24. Resnicoff M, Medrano EE, Podhajcer OL, Bravo AI, Bover L, Mordoh J (1987) Subpopulations of MCF7 cells separated by Percoll gradient centrifugation: a model to analyze the heterogeneity of human breast cancer. Proc Natl Acad Sci USA 84(20):7295–7299
25. Folch J, Lees M, Sloane Stanley GH (1957) A simple method for the isolation and purification of total lipides from animal tissues. J Biol Chem 226(1):497–509
26. Aloisi JD SJ, Fried B (1990) Quantification of lipids by one-dimensional TLC on Preadsorbent High Performance Silica Gel Plates J Liq Chrom Relat Tech 13 (20):3949–3961
27. Sterin-Speziale N, Kahane VL, Setton CP, Fernandez MC, Speziale EH (1992) Compartmental study of rat renal phospholipid metabolism. Lipids 27(1):10–14
28. Samsa MM, Mondotte JA, Iglesias NG, Assuncao-Miranda I, Barbosa-Lima G, Da Poian AT, Bozza PT, Gamarnik AV (2009) Dengue virus capsid protein usurps lipid droplets for viral particle formation. PLoS Pathog 5(10):e1000632. doi:10.1371/journal.ppat.1000632
29. Bradford MM (1976) A rapid and sensitive method for the quantitation of microgram quantities of protein utilizing the principle of protein-dye binding. Anal Biochem 72:248–254
30. Kruth HS (1984) Localization of unesterified cholesterol in human atherosclerotic lesions. Demonstration of filipin-positive, oil-red-O-negative particles. Am J Pathol 114(2):201–208
31. Kuhajda FP (2000) Fatty-acid synthase and human cancer: new perspectives on its role in tumor biology. Nutrition 16(3):202–208
32. De Maziere AM, Muehlethaler K, van Donselaar E, Salvi S, Davoust J, Cerottini JC, Levy F, Slot JW, Rimoldi D (2002) The melanocytic protein Melan-A/MART-1 has a subcellular localization distinct from typical melanosomal proteins. Traffic 3(9):678–693
33. Steinman RM, Gutchinov B, Witmer MD, Nussenzweig MC (1983) Dendritic cells are the principal stimulators of the primary mixed leukocyte reaction in mice. J Exp Med 157(2):613–627
34. Jonuleit H, Kuhn U, Muller G, Steinbrink K, Paragnik L, Schmitt E, Knop J, Enk AH (1997) Pro-inflammatory cytokines and prostaglandins induce maturation of potent immunostimulatory dendritic cells under fetal calf serum-free conditions. Eur J Immunol 27(12):3135–3142. doi:10.1002/eji.1830271209
35. Toh HC, Wang WW, Chia WK, Kvistborg P, Sun L, Teo K, Phoon YP, Soe Y, Tan SH, Hee SW, Foo KF, Ong S, Koo WH, Zocca MB, Claesson MH (2009) Clinical benefit of allogeneic melanoma cell lysate-pulsed autologous dendritic cell vaccine in MAGE-positive colorectal cancer patients. Clin Cancer Res 15(24):7726–7736. doi:10.1158/1078-0432.CCR-09-1537
36. Walther TC, Farese RV Jr (2009) The life of lipid droplets. Biochim Biophys Acta 1791(6):459–466. doi:10.1016/j.bbalip.2008.10.009
37. Murphy DJ (2001) The biogenesis and functions of lipid bodies in animals, plants and microorganisms. Prog Lipid Res 40(5):325–438
38. Accioly MT, Pacheco P, Maya-Monteiro CM, Carrossini N, Robbs BK, Oliveira SS, Kaufmann C, Morgado-Diaz JA, Bozza PT, Viola JP (2008) Lipid bodies are reservoirs of cyclooxygenase-2 and sites of prostaglandin-E2 synthesis in colon cancer cells. Cancer Res 68(6):1732–1740. doi:10.1158/0008-5472.CAN-07-1999
39. Swinnen JV, Brusselmans K, Verhoeven G (2006) Increased lipogenesis in cancer cells: new players, novel targets. Curr Opin Clin Nutr Metab Care 9(4):358–365. doi:10.1097/01.mco.0000232894.28674.30
40. Kuhajda FP (2006) Fatty acid synthase and cancer: new application of an old pathway. Cancer Res 66(12):5977–5980. doi:10.1158/0008-5472.CAN-05-4673
41. Bozza PT, Viola JP (2010) Lipid droplets in inflammation and cancer. Prostaglandins Leukot Essent Fatty Acids 82(4–6):243–250. doi:10.1016/j.plefa.2010.02.005
42. Bostrom P, Andersson L, Rutberg M, Perman J, Lidberg U, Johansson BR, Fernandez-Rodriguez J, Ericson J, Nilsson T, Boren J, Olofsson SO (2007) SNARE proteins mediate fusion between cytosolic lipid droplets and are implicated in insulin sensitivity. Nat Cell Biol 9(11):1286–1293. doi:10.1038/ncb1648
43. Al-Saffar NM, Titley JC, Robertson D, Clarke PA, Jackson LE, Leach MO, Ronen SM (2002) Apoptosis is associated with triacylglycerol accumulation in Jurkat T-cells. Br J Cancer 86(6):963–970. doi:10.1038/sj.bjc.6600188
44. Exton JH (1994) Phosphatidylcholine breakdown and signal transduction. Biochim Biophys Acta 1212(1):26–42
45. Liao YP, Wang CC, Butterfield LH, Economou JS, Ribas A, Meng WS, Iwamoto KS, McBride WH (2004) Ionizing radiation affects human MART-1 melanoma antigen processing and presentation by dendritic cells. J Immunol 173(4):2462–2469